RSC Advances

PAPER

View Article Online
View Journal | View Issue

Cite this: *RSC Adv.*, 2024, **14**, 779

Investigation of the *in vitro* biological activities of polyethylene glycol-based thermally stable polyurethane elastomers

Nadia Akram, *[a] Muhammad Shahbaz,[a] Khalid Mahmood Zia,[a] Muhammad Usman,[a] Akbar Ali, *[a] Rashad Al-Salahi, [b] Hatem A. Abuelizz [b] and Cédric Delattre [cd]

The intense urge to replace conventional polymers with ecofriendly monomers is a step towards green products. The novelty of this study is the extraction of starch from the biowaste of wheat bran (WB) and banana peel (BP) for use as a monomer in the form of chain extenders. For the synthesis of polyurethane (PU) elastomers, polyethylene glycol (PEG) bearing an average molecular weight $M_n = 1000$ g mol^{-1} was used as a macrodiol, which was reacted with isophorone diisocyanate (IPDI) to develop NCO-terminated prepolymer chains. These prepolymer chains were terminated with chain extenders. Two series of linear PU elastomers were prepared by varying the concentration of chain extenders (0.5–2.5 mol%), inducing a variation of 40 to 70 wt% in the hard segment (HS). Fourier-transform infrared (FTIR) spectroscopy confirmed the formation of urethane linkages. Thermal gravimetric analysis (TGA) showed a thermal stability of up to 250 °C. Dynamic mechanical analysis (DMA) revealed a storage modulus (E') of up to 140 MPa. Furthermore, the hemolytic activities of up to 8.97 ± 0.1% were recorded. The inhibition of biofilm formation was investigated against *E. coli* and *S. aureus* (%), which was supported by phase contrast microscopy.

Received 14th October 2023
Accepted 8th December 2023

DOI: 10.1039/d3ra06997d

rsc.li/rsc-advances

1. Introduction

The polymer industry is flourishing at its peak, with mainly utilizing petrochemical raw materials for the production of polymers in all fields, including electronics, transportation, packaging, and medicine. However, petrochemical raw materials are expensive and a potential threat to the environment. The environmental legislations encourage the development of renewable resources to replace conventional petroleum-based polymers in order to minimize the issues of economy and pollution.[1,2] As petroleum-based polymers are excessively used in various industrial sectors, the accumulation of these materials in the eco-system cannot be avoided. Hence, the only choice to overcome this problem is the treatment for petroleum-based polymers. Recycling seems to be a reliable solution to keep the material in the circular economy.[3] Bio-based polymers are a preferred choice to resolve the economic and environmental concerns related to conventional petroleum-based polymers. These bio-based polymers can be synthesized either as a whole or as a fragment incorporated with petroleum-based polymers, making a strong environment-friendly impact.[4] Polyurethane (PU) is a versatile class of polymers consisting of repeated urethane linkage, which is obtained by the addition reaction between polyol and diisocyanate. PU consists of alternate hard segments (HS) and soft segments (SS).[5] The "SS" is defined as the portion of macrodiol contributing to the final polymer chains, whereas the "HS" is defined as the portion obtained by the components of diisocyanates and chain extenders. The properties of the final product can be tuned based on the chemical structure, composition, and molecular weight of the monomers.[6]

PU can either be linear or cross-linked based on the availability of the functional groups of the monomers.[7] The renewable resources are comparable with petroleum-based polymers in their properties and offer environment-friendly products with distinctive structures and excellent characteristics.[8] Among the available renewable resources, starch has shown consistent results owing to its multivariant features as it possess biodegradable and biocompatible properties.[9] Bio-based polymers are eco-friendly materials, and their chemical versatility, sustainability, biocompatibility and biodegradability make them potentially suitable for various applications, including in food, electronics, agriculture, textile, biomedical, and cosmetic industries.[10,11] The selection of starch or other bio-based polymers is primarily because of the huge impact of the food

[a]*Department of Chemistry, Government College University Faisalabad, Faisalabad-38000, Pakistan. E-mail: nadiaakram@gcuf.edu.pk; akbarali@gcuf.edu.pk*

[b]*Department of Pharmaceutical Chemistry, College of Pharmacy, King Saud University, Riyadh 11451, Saudi Arabia*

[c]*Université Clermont Auvergne, Clermont Auvergne INP, CNRS, Institut Pascal, F-63000 Clermont-Ferrand, France*

[d]*Institut Universitaire de France (IUF), 1 Rue Descartes, 75005 Paris, France*

industry in the market. Although the food industry is currently confronting a wide range of difficulties in ensuring the quality of food with a longer shelf life and long-term preservation, it is also one of the major industries for the production of biowaste. The industries have been able to tackle these issues to develop sustainable and biodegradable food packaging materials based on biopolymers. Additionally, because of their superior biodegradability, renewability, bioavailability, and non-toxicity, these eco-friendly materials are reducing the environmental issues connected to plastic-related pollution.[12] The starch modification allows for the thermal stability, mechanical properties, and the biocompatibility of the polymers.[13,14] Starch is an abundantly available and inexpensive polysaccharide which can be obtained from numerous resources, including corn, wheat grains, cassava, nuts, potato, rice *etc.* In its basic structure, D-glucose units are connected by α-1 to 4 or α-1 to 6 glycosidic linkages.[15] Due to the availability of starch from various resources, the choice of the sources is significant. Wheat is one of the major sources of food all over the world. The processing of its grains leaves the wheat bran (WB) as biowaste, which still contains significant quantity of starch and other nutrients.[14] Its consumption is increasing day-by-day in the form of animal's feed.[15,16] Hence, it is the most suitable, bio-based, and cheap source of starch which is available as biowaste.

Apart from wheat, another abundantly available food is banana fruit. The weight of banana peel (BP) is nearly 40 percent of the total weight of banana.[17] Peels are thrown in municipal waste, which causes environment pollution and air contamination. The trend of using BP is increasing nowadays in different kinds of applications in industry, including the production of bio-based fuel, energy production, cosmetics production, fertilizer, for cleaning of the environment.[18] The BP (not too ripened) is a rich source of starch, which is approximately 22.5%.[19–23] Due to its mass production, it is considered an important source of biowaste as the continuously increased consumption of synthetic polymers is the primary cause of the pollution. Even today, different non-degradable materials (including stainless steel (SS), titanium, and chromium–cobalt (Cr–Co) alloys) are extensively employed as temporary or permanent implanting materials.[24] Researchers have paid great attention to probe the natural fibers and biomaterials for the replacement of petroleum-based polymers. The nature of the reinforcement has the ability to induce superior characteristics in the new materials. Unfortunately, there is still limited data available to utilize the bio-based materials. The majority of the available data has been explored in pilot-scale research only, making it scarcely possible for use in engineering applications.[25] Researchers have reported numerous biomaterials, which showed better properties of the final products. Sudhakar and coworkers have reported the applications of seaweed biopolymers and composites in dental applications.[26] Muthiyal and Purushothaman have reported on the fabrication and characterization of stimuli-responsive scaffold/bio-membrane using a novel carrageenan biopolymer for biomedical applications.[27] Sachin and Jyoti have also reported on seaweed-based biodegradable biopolymers, composites, and blends with applications in bioremediation using weeds.[28] Freile and coworkers used biodegradable polymer blends and composites from seaweeds.[29] Sudhakar and coworkers worked on the fabrication and characterization of bio-nanocomposite films using κ-Carrageenan and *Kappaphycus alvarezii* seaweed for multiple industrial applications.[30] Akram *et al.* have reported on the fabrication of chitosan-reinforced polyurethanes.[31] Marta and coworkers have reported on the properties, modification and applications of banana starch.[32] Jana and coworkers have provided details about the wheat starch structure–function relationship in bread making.[33] Kim has presented an understanding of the wheat starch metabolism in its properties, environmental stress condition, and molecular approaches for value-added utilization.[34]

The conversion of petroleum-based polymers into bio-based polymers can be achieved by the addition of bio-components. However, the biowaste of the natural sources can also provide an adequate source to convert the synthetic petroleum-based polymers into bio-based polymers. The novelty of this work is the extension of PU chains with starch, which have been derived from WB and BP. Hence, the chain extender is basically derived from biowaste material. This approach is a step towards a green environment. The product based on biowaste materials can provide a good option of recycling and degradation. Although some researchers have reported on the work with starch-induced polyurethane composites, none have utilized the biowaste materials for the purpose of recycling, which is the novelty of this work. In this regard, Zia *et al.*[35] presented a review article of starch-based polyurethanes. Tai *et al.*[36] used hexamethylene diisocyanate and high amylose starch (HAGS). Similarly, Gürses *et al.*[37] have synthesized aliphatic diisocyanate and saccharides-based polyurethane composites. This brief review also suggests that the recycling of biowastes as new monomers is an area with great potential of being explored and utilized as a step towards achieving a green environment, as addressed in this article.

Hence, the aim of this work is to draw the attention of researchers to extract components from biowaste materials, and to utilize them for the fabrication of elastomers. It will not only produce an economic and ecological-friendly product, but it will also help to discover new varieties of biowaste materials for the useful purpose. In order to utilize the biowaste, starch was extracted as a monomer. As the researchers have reported that the chemical compositions, molecular structure and morphology of starches are unique for each particular plant species based on their quantitative and qualitative nature, the various types of starch can induce various properties. In order to evaluate the impact of starch as a monomer from the two different biowastes, *i.e.*, wheat bran and banana peel, two series of PU elastomers were synthesized with the systematic variation of stoichiometry. Polyethylene glycol (PEG) as a macrodiol was reacted with isophorone diisocyanate (IPDI). The prepolymer chains were terminated using starch from both biowastes in two separate series. Five samples were prepared in each series with varying hard segment contents. All of the synthesized samples were subjected to structural, thermal, mechanical, morphological and biological activities. The synthesized samples were also subjected to swelling behavior.

2. Materials and methods

2.1. Chemicals

The following chemicals have been used in their pure form for the synthesis of the PU elastomer: polyethylene glycol (PEG) M_n = 1000 g mol^{-1} (Aldrich), isophorone diisocyanate (IPDI) (Aldrich), dibutyltin dilaurate (DBTDL) (Aldrich), sodium metabisulfite (Aldrich), sodium chloride, ethanol, and toluene. Wheat bran was collected from the wheat flour industry and banana peel was obtained from fresh seasonal banana. Macrodiol was demoisturized at 70 °C for 24 hours in a vacuum to evaporate any moisture contents and impurities. All of the reagents, chemicals and solvent were analytical grade, and used in the research work without further treatment.[38]

2.2. Extraction of starch from wheat bran (WB)

The WB powder obtained from the wheat flour industry was soaked in ethanol (70%) for 24 hours at ambient temperature to develop a slurry. The slurry was decanted to remove all of the dirt particles. It was again soaked in water and ground to reduce the particle size. The mixture was then sieved through a mesh. The residues were washed with water thrice, the resultant filtrate was centrifuged at 3000 rpm, and the starch cake was obtained. Washing of the protein fraction from the starch granules was performed by adding NaCl solution into the starch with continuous stirring. The solution was then centrifuged again to obtain the starch sediments. Starch sediments were added in a separating flask containing the water/toluene solution, and were shaken well. The layer of water containing starch was collected. The layer of toluene containing protein was again mixed in water, and shaken well. The layers of water and toluene containing starch and protein, respectively, were collected. This process was repeated up to three or four times to extract all of the starch. Finally, all of the layers of water containing starch were collected and centrifuged to obtain starch. The flow sheet diagram for the extraction process is given in Fig. 1A.

2.2.1. Extraction of starch from banana peel (BP). The weighted quantity (25 g) of peel was taken into small pieces and washed with distilled water. The peels were soaked into a 30% solution of sodium metabisulphite in distilled water. The mixture was homogenized and filtered by using filter cloth. In order to settle starch sediments, the filtrate was kept for 24 hours, followed by decantation. The collected starch was then dried in an oven at 40 °C. The flow sheet diagram for the extraction of starch from banana peel is given in Fig. 1B.

2.2.2. Synthesis of the PU elastomers extended with wheat starch (WS) & banana starch (BS). For the synthesis of linear PU elastomers, the prepolymer method was adopted as described in detail in one of our publications.[5] In order to carry out the reaction, the synthetic assembly carrying a round-bottom flask was connected with a water inlet and out through reflux condenser. The flask was equipped with a mechanical stirrer and nitrogen inlet and thermometer. Pretreated PEG (M_n = 1000 g mol^{-1}) as the macrodiol was taken into the round-bottom flask, and it was reacted with isophorone diisocyanate

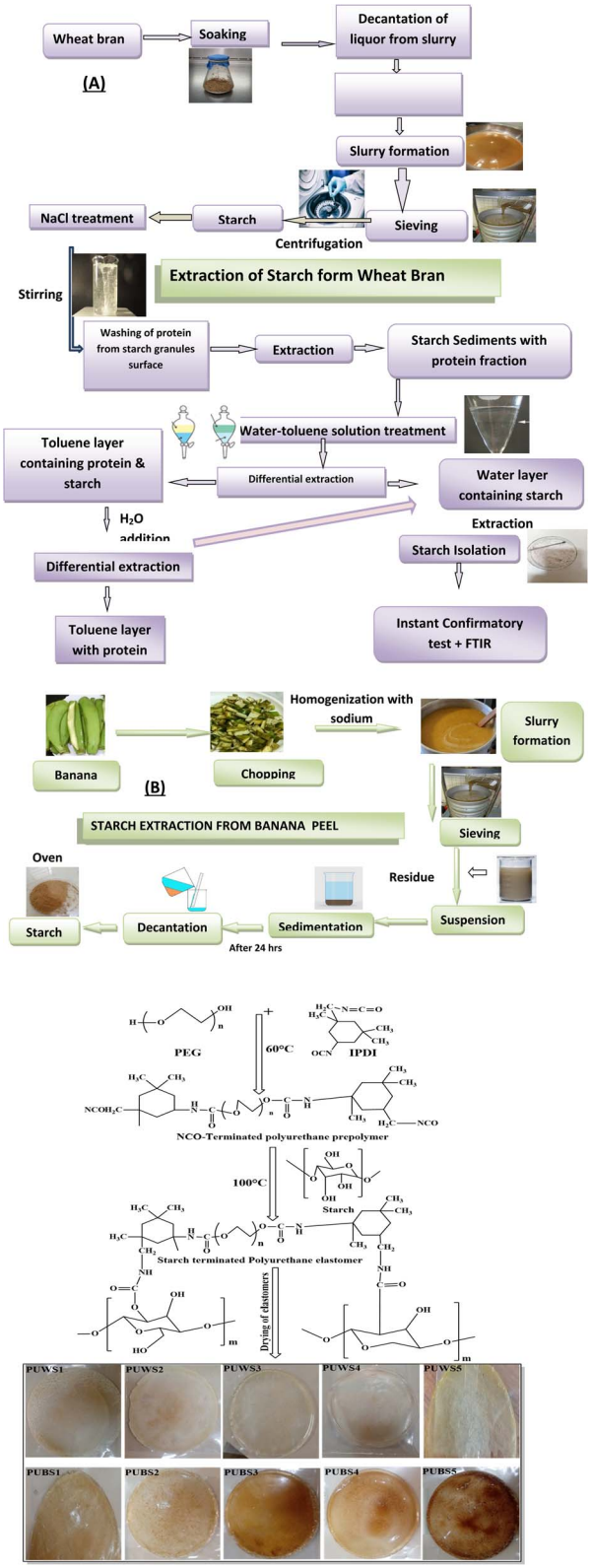

Fig. 1 Flow sheet depicting the extraction of starch from biowaste materials. (A) Systematic extraction of starch from wheat bran. (B) Systematic exaction of starch from banana peel. (C) Synthetic route for the synthesis of PU elastomers extended and terminated with wheat bran starch and banana peel starch, and original photographs of the synthesized samples.

Table 1 Sample code designations and molar compositions of two series of polyurethane elastomers[a]

Theoretical stoichiometry of series I-PUWS				Theoretical stoichiometry of series II-PUBS			
Sample code	Polyol : diisocyanate : starch as (CE) (mol%)	HS	SS	Sample code	Polyol : diisocyanate : starch as (CE) (mol%)	HS	SS
PUWS1	1 : 3 : 0.5	40.25	59.75	PUBS1	1 : 3 : 0.5	40.25	59.75
PUWS2	1 : 5 : 1	52.91	47.09	PUBS2	1 : 5 : 1	52.91	47.09
PUWS3	1 : 6 : 1.5	62.9	37.10	PUBS3	1 : 6 : 1.5	62.9	37.10
PUWS4	1 : 9 : 2	66.4	33.06	PUBS4	1 : 9 : 2	66.4	33.06
PUWS5	1 : 11 : 2.5	72.75	27.25	PUBS5	1 : 11 : 2.5	72.75	27.25

[a] PUWS stands for the polyurethane elastomer chain extended with wheat bran starch, and PUBS stands for the polyurethane elastomer chain extended with banana peel starch, the numbers 1–5 represent the systematic variation in the compositions of all samples.

(IPDI). Dibutyltin dilaurate (DBTDL) was used as a catalyst, which produced the NCO-terminated prepolymer chains. In order to extend the polymer chains, starch extracted from WB was used as a chain extender. The acetone was used as a solvent in order to maintain the viscosity of the samples. For drying, the synthesized samples were dispensed into the molds of polytetrafluoroethylene (PTFE). A short time (10 min) swift venting was performed under vacuum at room temperature. The complete drying was carried out in 72 h. The thickness of the dried films (2 ± 0.05 mm) was determined by digital calipers. The same protocol was adopted for the synthesis of PU elastomers using banana peel starch as the chain extenders. Two series of linear PU elastomers were synthesized. The PU elastomers series obtained by using wheat bran starch and banana peel starch as the chain extender has been designated as PUWS and PUBS, respectively; each containing five samples with systematic variation in the concentration of monomers. Prior to analysis, all of the samples were stored in a desiccator. The synthetic route for the synthesis of PU samples has been given in Fig. 1C. All of the synthesized samples were subjected to structural, thermo-mechanical, morphological, solvent absorption and biological activity tests. The sample code designation, molar composition, HS and SS composition of all samples have been listed in Table 1.

2.3. Characterization

2.3.1. Fourier transform infrared spectroscopy (FTIR). FTIR is an analytical technique that is used to evaluate the functional groups and linkage present in an organic or inorganic compound by the absorption of IR radiation in the specific frequency range of 4000–400 cm^{-1}. PU elastomers were subjected to FTIR analysis using a NICOLET 6700 spectrometer containing attenuated total reflectance (ATR) as an accessory. All of the spectra were documented in transmission mode under N_2 atmosphere at 25 °C. The scan rate was in the range of 4000–400 cm^{-1} using % transmittance mode.

2.3.2. Thermal gravimetric analysis (TGA). TGA is defined as the mode of thermal analysis, where the mass of a sample is evaluated w.r.t. the change in temperature. All of the thermal analysis was recorded using a PerkinElmer's Thermogravimetric Analyzer (TGA), (Waltham, Massachusetts, USA). The analysis was performed at the ramp rate of 10 °C min^{-1} under N_2 atmosphere with a flow rate of 50 mL min^{-1}. The analysis was carried out in the temperature range of 50 °C to 600 °C.[2–5]

2.3.3. Swelling test. The solvent intake ability of the synthesized samples was carried by performing the swelling test. The PU elastomers were soaked in distilled H_2O and DMSO to assess the variation in their weight change (%) until a persistent weight was recorded. The swelling tendencies in both solvents were calculated using equation.[1]

$$\%\ \text{water/DMSO absorption} = \frac{\text{wet weight} - \text{dry weight}}{\text{total weight}} \times 100 \quad (1)$$

2.3.4. Biological activity tests

2.3.4.1. Hemolytic activity. Hemolytic activity is defined as the tendency of the bacterium to break down red blood cells (RBCs) in order to release the hemoglobin (Hb). The hemolytic activity of the PU elastomers was performed by using a screw-cap tube, which was made up of polystyrene.[39,40] The fresh 5 mL heparinized human blood was poured into the tube, and it was centrifuged for 5.0 minutes at 850 rpm. The obtained supernatant was decanted off, while the viscid pellets were washed with phosphate buffer saline (PBS) (pH ~ 7.4). After thoroughly washing the pellets three times with the PBS, it was suspended in approximately 20 mL PBS. The cell suspension was placed on ice, which was later diluted with PBS for analysis. A fraction of PU elastomer (20 μL) was immersed into a microfuge tube (2.0 mL), and the cell suspensions (180 μL) in the diluted condition was homogenously mixed. The PBS was used as a negative control in analysis, while the Triton X-100 (0.1%) was used as a positive control. The Eppendorf tubes were instantly centrifuged for ten minutes. The supernatant (100 μL) was collected using microfuge tubes, which were sterilized prior to collection. The supernatant was diluted with PBS (900 μL), making three replicate of each supernatant (200 μL). It was then shifted into a sterile 96-well microplate containing one positive and negative control. The absorbance was recorded at 540 nm on a microplate reader (BioTek, USA). Hemolysis (%) of each sample was calculated using eqn (2).[41]

$$\text{Hemolysis}\ (\%) = \frac{\text{sample absorbance} - \text{negative control}}{\text{positive control}} \times 100 \quad (2)$$

2.3.4.2. Biofilm inhibition assay. This test is performed to evaluate the ability of the polymers to inhibit the bacterial growth. *Staphylococcus aureus* (*S. aureus*) and *Escherichia coli* (*E. coli*) were used to evaluate the biofilm inhibition activity, as reported earlier by the researchers.[42,43] For this purpose, a sterile plastic tissue culture 96-well plate with a flat bottom was filled with 100 μL of nutrient broth (Oxford, UK), and 100 μL each of the PU elastomer suspensions were inoculated with a bacterial suspension of 20 μL into the wells separately. The bacteria and its nutrient broth without PU suspension in wells acted as the control for both strains (10 μg/20 μL). The 96-well plate was covered and incubated at 37 °C for 24 hours in a temperature-controlled incubator in aerobic conditions. Ciprofloxacin was used as a standard (positive control) to compare the PU elastomers results. After incubation, each well was washed thrice with sterile phosphate buffer (220 μL to each well). To remove the non-adherent bacteria from wells, the plate was shaken well. After washing, to fix the attached bacteria, 99% methanol (220 μL per well) was added and left for 15 minutes. After that, methanol was discarded and left to dry. To stain, 220 μL of 2% crystal violet was added to each well for 5 minutes. To remove excess stain, the plate was rinsed under running tap water and air dried at room temperature. The dye bound to the adhered cells was re-solubilized with 220 μL of 33% (v/v) glacial acetic acid in each well. Using a micro-plate reader (BioTek, USA), the optical density was measured for each well at 630 nm. The bacterial growth inhibition percentage (INH%) was calculated using eqn (3).

$$1\mathrm{NH}(\%) = 1 - \frac{\mathrm{OD630\ (sample)}}{\mathrm{OD630\ (control)}} \times\ 100\% \qquad (3)$$

2.3.4.3. Biofilm inhibition through phase contrast microscopy. Phase contrast microscopy is defined as an optical microscopic technique, which has the potential to translate phase shifts in light when passed through a clear sample to brightness variations in the image. The biofilm inhibition tendency of the PU elastomers of the selected samples was also observed by using Phase contrast microscopy.[44] For this purpose, a few droplets of *S. aureus* and *E. coli* were cultured on glass slides and incubated at 37 °C for 14 h. The slides were washed with PBS. After the washing of the slides, they were immersed in the PU elastomer suspension. The slides were rinsed, stained and the biofilms were dissolved using 30% glacial acetic acid. Negative PBS control slide and positive control slide with ciprofloxacin were also prepared without PU elastomer suspensions. All of the prepared glass slides were examined microscopically.

2.3.5. Dynamic mechanical analysis (DMA). DMA is a technique which is used to determine the viscoelastic properties of the polymers. For DMA analysis, the samples were used in the following dimensions: length; 50 mm, width; 2.5 mm, Thickness 1–2 ± 0.5 mm. The analysis was performed on DMA (Q800; TA Instruments, New Castle, DE) in temperature sweep mode. The values of the storage modulus (E') and damping factor (tan δ) were recorded.

3. Results and discussion

3.1. Confirmation of the linkages of the PU elastomers by FTIR analysis

The FTIR spectra of all the monomers, prepolymers and representative spectra of PU elastomers of both series PUWS and PUBS are given in Fig. 2. The characteristic main peaks of the spectra are listed in Table 2. A band at 2857–2960 cm^{-1} appeared, which was due to the C–H symmetric and asymmetric vibrations. The band for N–H stretching was observed at 1556 cm^{-1}. A band for urethane C=O was present at 1631 cm^{-1}. Furthermore, the high intensity bands of the NCO and OH groups were diminished, which provided the indication of a reaction between PEG and IPDI and the formation of the pre-polymer. Other functional groups were also observed, such as the C=O stretching (1717 cm^{-1}), bending vibrations of the CH_3 group (1456 cm^{-1}), stretching C–O vibration of the urethane group (1089 cm^{-1}) and others. The pre-polymer was reacted with starch (chain extender) to obtain the final polyurethane. The FTIR spectra of both kinds of starch showed a broad peak for the OH group present in the range of 3450–3100 cm^{-1}, which has confirmed the hydrogen bonding present in starch. The peaks of absorption at 2941–2650 cm^{-1} were due to the symmetric and asymmetric vibrations of the CH_3 group. The stretching vibration band for C–O–C was observed at 1010–984 cm^{-1}. The band of NCO disappeared and the band for N–H appeared between 3508–3340 cm^{-1}, which confirmed the

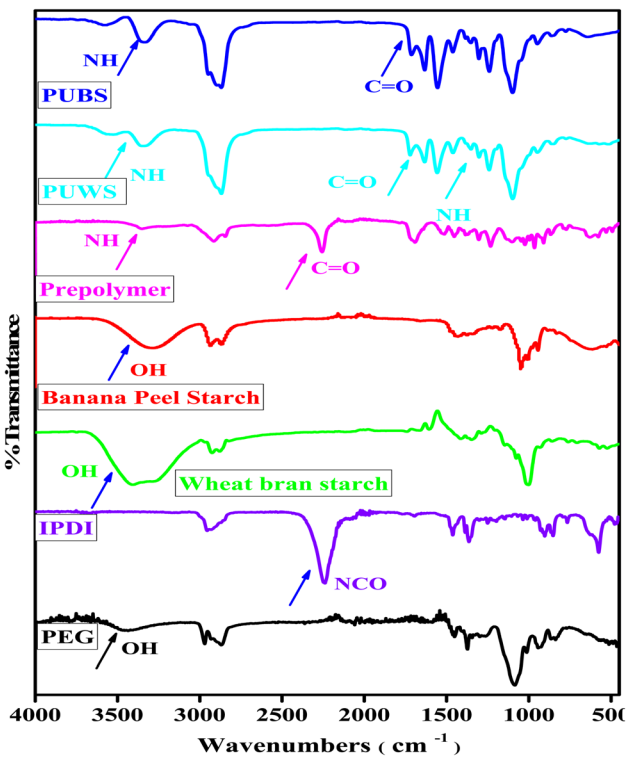

Fig. 2 Representative FTIR spectra of all of the monomers: polyethylene glycol (PEG), isophorone diisocyanate (IPDI), banana peel starch, Wheat bran peel starch, prepolymer, and PU elastomers based on wheat bran starch (PUWS)and banana peel starch (PUBS).

Table 2 FTIR peak assignments for the polyurethane elastomers

Assignments	Wavenumber (cm^{-1}) Observed value range of different groups of samples	Wavenumber (cm^{-1}) Literature values[2,8,14,22]
N–H (str)	3442–3351	3400–3325
CH_2 (sym)	2882–2867	2880–2860
CH_2 (Asym)	2954–2882	2970–2880
C=O (str)	1740–1709	1750–1700
N–H (bend)	1631–1549	1650–1550
C–H (wag)	960–940	970–960
C–O	1124–1096	1140–1070

formation of the finally prepared polymer. Other peaks for the carbonyl stretching were found between 1760–1710 cm^{-1}, C–O–C (1100 cm^{-1}), and the bending vibrations of methylene (1458 cm^{-1}). Hence, all of the bands that appeared confirmed the reaction completion and synthesis of the final PU elastomers. The stoichiometry of the compositions shows that all of the monomers have the optimum chance to react with each other. This is the most likely result, which is expected from the condensation polymerization.

3.2. Estimation of thermal stability of PU elastomers by TGA

The thermal stability of individual monomers plays a significant role in the stability of the final polymer. Usually, it is complicated to evaluate the thermal behavior of Pus due to the involvement of various monomers containing different functional groups. These functional groups generate the desired chemical linkage. During this process, the breaking of the parent chemical bonds and development of the daughter chemical bonds takes place, releasing gaseous products as well. The TGA curves of all of the elastomers are presented in Fig. 3. The stepwise degradation is reported in Table 3. For the PUWS series, multicurves were observed with the thermal stability in the range of 280 °C. The increase in the thermal stability was due to an increase in the concentration of starch, indicating that the composites are better in their thermal behavior as compared to the neat polymers. A similar range of thermal stability of biocompatible PU elastomers was also reported by Chen *et al.*[45] for skeletal muscle and tissue engineering applications. No extra peaks have been observed, which has ruled out the presence of byproducts. The guarantee of unreacted monomers is the reaction sensitivity of all the monomers especially diisocyanates, which will react with the atmospheric OH group in the case of unavailability of the OH groups from the monomers. This may result in the production of urea and carbon dioxide as a by-product. However, as the stoichiometry is well defined, no such products have been observed and only linear products have been observed as depicted from the data of TGA. The prominent transition in the. PU elastomers were observed in the range of 300 °C, leading to a continuous decrease in weight loss up to 60 wt%. A similar behavior was observed for another transition around 350 °C depicting a slight variation in the thermal stability throughout the series, whereas the maximum weight loss was observed up to 440 °C. The

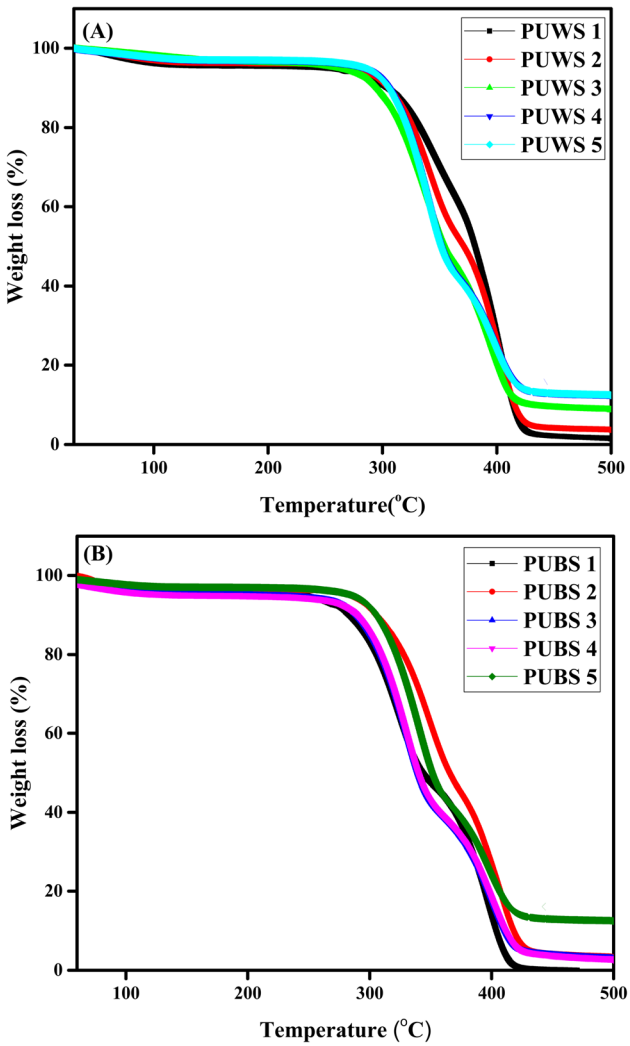

Fig. 3 TGA curves of all the synthesized samples of PU elastomers. (A) TGA curves of the PUWS series chain extended with wheat bran starch. (B) TGA curves of the PUBS series chain extended with banana peel starch.

similar trend was also observed for the PUBS series as well, where the maximum weight loss was observed up to 425 °C. The first stage of degradation has indicated the loss of hydroxyl contents induced by the starch. It is also important that the requirement of thermal stability varies according to applications, and elastomers have the ability to mediate such applications for thermal behavior. In the case of PU elastomers, the observed thermal stability is within the usual range of elastomeric applications. The similar range of thermal stability has also been reported by Parcheta *et al.*[46] for green PU elastomers. The 2nd major stage of degradation (250–350 °C) was observed due to the breakdown of the urethane linkage, leading to the ultimate weight loss of the samples. The last stage of degradation was due to the presence of a long chain of hydrocarbons induced by the PEG as the macrodiol. The data revealed that the addition of starch as a biocomponent has improved the thermal stability significantly. The synthesized starch-induced PU elastomers have shown a comparable thermal stability with the petroleum-based polymers.

Table 3 Weight loss (%) data obtained by TGA and swelling tendency of PU elastomers

Sample code	T@10% wt. loss (°C)	T@20% wt. loss (°C)	T@50% wt. loss (°C)	T @Maximum wt. loss (°C)	H_2O absorption tendency (%)	DMSO absorption tendency (%)	Sample code	T@10% wt. loss (°C)	T@20% wt. loss (°C)	T@ 50% wt. loss (°C)	T@ % wt. loss maximum (°C)	H_2O absorption tendency (%)	DMSO absorption tendency (%)
PUWS1	304.4	332.9	380.9	426.6	27 ± 0.3	28 ± 0.9	PUBS1	295.6	317.0	373.1	423.4	25 ± 0.5	27 ± 0.9
PUWS2	303.6	324.9	370.7	426.0	36 ± 0.2	38 ± 0.8	PUBS2	282.6	305.8	343.1	425.9	33 ± 0.7	37 ± 0.8
PUWS3	297.6	318.5	362.9	423.3	46 ± 0.2	48 ± 0.8	PUBS3	289.8	309.3	339.6	334.4	44 ± 0.8	47 ± 0.8
PUWS4	293.7	316.8	354.2	440.6	50 ± 0.2	52 ± 0.7	PUBS4	288.8	310.1	339.0	435.2	47 ± 0.9	51 ± 0.7
PUWS5	304.7	322.4	350.9	335.7	84 ± 1.0	88 ± 1.0	PUBS5	307.9	323.4	351.5	431.5	75 ± 1.0	86 ± 1.5

3.3. Solvent absorption tendency of PU elastomers by swelling test

The polymers show different interactions based on their nature and aptitude towards solvents. The behavior of the PU elastomers of both series PUWS and PUBS in water and DMO is shown in Fig. 4. The architecture of the PU shows the polar and non-polar groups in the main chain. Whenever the concentration of polar or non-polar segment is in excess, the solvent absorption tendency varies. Each segment of the PU decides on the overall behavior of the polymer. The long chains of the PEG as the macrodiol induce the nonpolar character, which appeared as SS in the chains. The urethane linkage developed by the diisocyanate and chain extender is polar in nature. Thus, the addition of PU elastomers in the water has shown a tendency to absorb water. The same results have also been observed with DMSO. This has satisfied the idea of water and solvent absorption in the case of PU elastomers. Water entered the samples and penetrated the chains of the polymers, which resulted in the weakness of bonds. Water absorption was rapid at start, and there was a rapid increase in weight gain in the first 2–3 hours. Then, the water penetration decreased to a minimum amount, and at last, there was no further increase in weight. As the concentration of starch was increased in the samples, they became more hydrophilic. The increase in starch contents in polyurethane increased the hard segments, and also increased the hydrophilicity of the samples, so the uptake of water was increased. Researchers have also reported that the swelling power was associated with the amylose content. The high amylose shows a strong structural network since the crystalline structure has a strong linkage and it restricts swelling.[47–49] The starch has the ability to entrain water and provide a sink for water. Researchers have also expressed it by changes in the food products. Furthermore, the swelling power is observed to be different from the syneresis that follows when water is expelled from the swollen starch granules or by other

Fig. 4 The swelling behavior of the PUWS series chain extended with wheat bran starch and the PUBS series chain extended with banana peel starch in H_2O and DMSO.

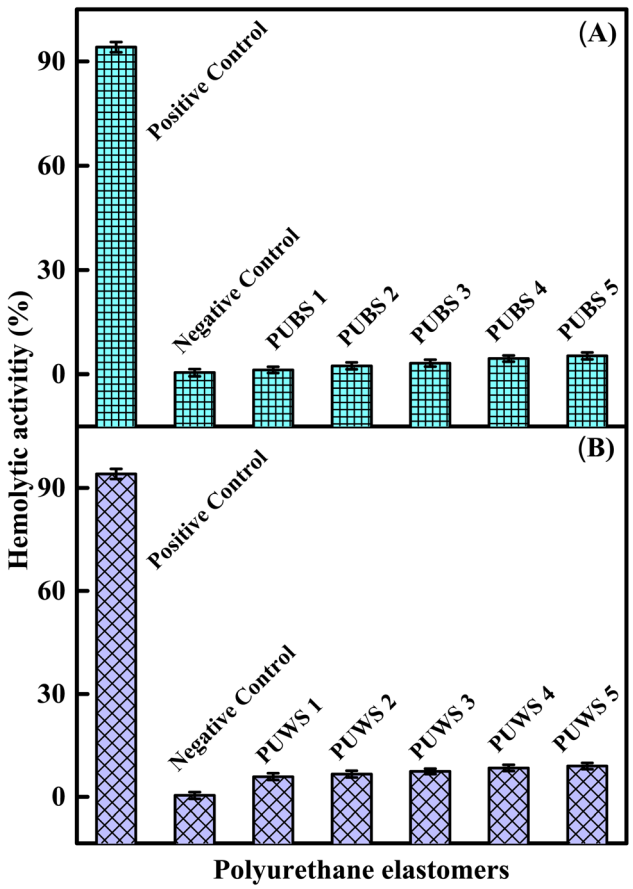

Fig. 5 Hemolytic activity of the PU elastomers. (A) Hemolytic activity of the PUWS series chain extended with wheat bran starch. (B) Hemolytic activity of PUBS series chain extended with banana peel starch.

ingredients.[50] This swelling power determines the quality of starch granules, and it is also based on the starch variety.[51] The reported values of the water absorption capacity vary from 130.45% to 251%. Moreover, some processes such as acetylation also increases the swelling tendency of starch. Hydroxypropylated banana starch has a higher granule swelling capacity and solubility compared to the native banana starch. The increase in granule swelling and solubility was also reported by several previous studies. The increasing granular swelling and solubility of the hydroxypropylated starch might be due to the starch granules becoming more hydrophilic because of the incorporation of the hydroxypropyl groups.[52,53]

3.4. Investigation of *in vitro* biological activities

3.4.1. Hemolytic assay of PU elastomers. The hemolytic activity of the synthesized samples of PU elastomers is given in Fig. 5. The hemolysis involves the rupturing of red blood cells (RBC). The tendency of the PU elastomers in terms of membrane damaging was quantified by the release of hemoglobin. The analysis has been performed to evaluate the hemolytic activity of the synthesized samples. The triton-X 100 was used as a positive control, which showed the lysis value as

Table 4 Bioassay data of the polyurethane elastomers

Sample code	Hemolytic activity (%)	Inhibition of biofilm formation against *E. coli* (%)	Inhibition of biofilm formation against *Staphylococcus aureus* (%)	Sample code	Hemolytic activity (%)	Inhibition of biofilm formation against *E. coli* (%)	Inhibition of biofilm formation against *Staphylococcus aureus* (%)
PUWS1	5.88 ± 0.1	20.28 ± 0.4	3.86 ± 0.5	PUBS1	1.17 ± 0.09	15.45 ± 0.2	15.45 ± 0.4
PUWS2	6.64 ± 0.2	22.69 ± 0.3	11.5 ± 0.4	PUBS2	2.35 ± 0.2	17.34 ± 0.5	17.39 ± 0.3
PUWS3	7.41 ± 0.2	25.07 ± 0.4	14.97 ± 0.2	PUBS3	3.11 ± 0.09	18.11 ± 0.3	19.80 ± 0.2
PUWS4	8.42 ± 0.09	35.26 ± 0.5	21.25 ± 0.5	PUBS4	4.47 ± 0.2	20.69 ± 0.5	22.70 ± 0.5
PUWS5	8.97 ± 0.1	37.40 ± 0.8	25.60 ± 0.7	PUBS5	5.23 ± 0.1	25.12 ± 0.6	25.12 ± 0.8
Triton X-100 (positive control)	94.1 ± 0.28	—	—	Triton X-100 (positive control)	94.1 ± 0.28	—	—
PBS (negative control)	0.41 ± 0.10	—	—	PBS (negative control)	0.41 ± 0.10	—	—
Ciprofloxacin (positive control	—	82.65 ± 2.74	77.57 ± 2.37			82.65 ± 2.74	77.57 ± 2.37

(94.1 ± 3.93%), causing the maximum damage to erythrocytes as RBC. On the other hand, phosphate buffer saline (PBS) was used as the negative control, which showed the lysis as (0.41%) to erythrocytes as the RBC encountered the minimum damage. Triton-X 100 and phosphate buffer were used as a reference. As a quantitative measure, the compatibility of the PU elastomers has been reported in Table 4. The PUBS series have shown lower values of hemolytic activities at 1.17 ± 0.09 (%), as compared to the PUWS series at 5.88 ± 0.1 (%). The results have indicated that a slight toxic effect has been observed with the synthesized compositions of the PUBS series, which has not affected the stability of the erythrocyte membrane. Overall, the samples of both series have shown the values of lysis (%) to be within a safe zone; hence, providing the evidence that the elastomers of the PUBS and PUWS series are strong candidates of biocompatible applications. The elastomers with a lower concentration of starch 0.5 (mol%) have shown better hemolytic activities as compared to the rest of the samples of the series. The hemolytic activity is related to the architecture of the PU elastomer. Hence, the concentration of each component plays a significant role in deciding the safety of the synthesized material towards various applications. It also scrutinizes the extent of biocompatible material in the synthesized samples.

3.4.2. Biofilm inhibition of PU elastomers. The bacterial biofilm inhibition ability of the two series of PU elastomers were evaluated, and the findings are given in Table 4. Ciprofloxacin has been used as a standard, which has shown the biofilm inhibition activity of 77.57 ± 2.37% against *S. aureus* and 82.65 ± 2.74% against *E. coli*, respectively. For the PUWS series, the biofilm inhibition activity in the range of 20.28 ± 0.4 %to 37.40 ± 0.8% has been observed against *E. coli*, whereas the biofilm inhibition activity in the range of 3.86 ± 0.5% to 25.60 ± 0.7% has been observed against *S. aureus.* Meanwhile, in the case of the PUBS series, the biofilm inhibition activity has been observed in the range of 15.45 ± 0.2% to 25.12 ± 0.6% and 15.45 ± 0.4% to 25.12 ± 0.8 against *S. aureus* and *E. coli*, respectively. All of the PU

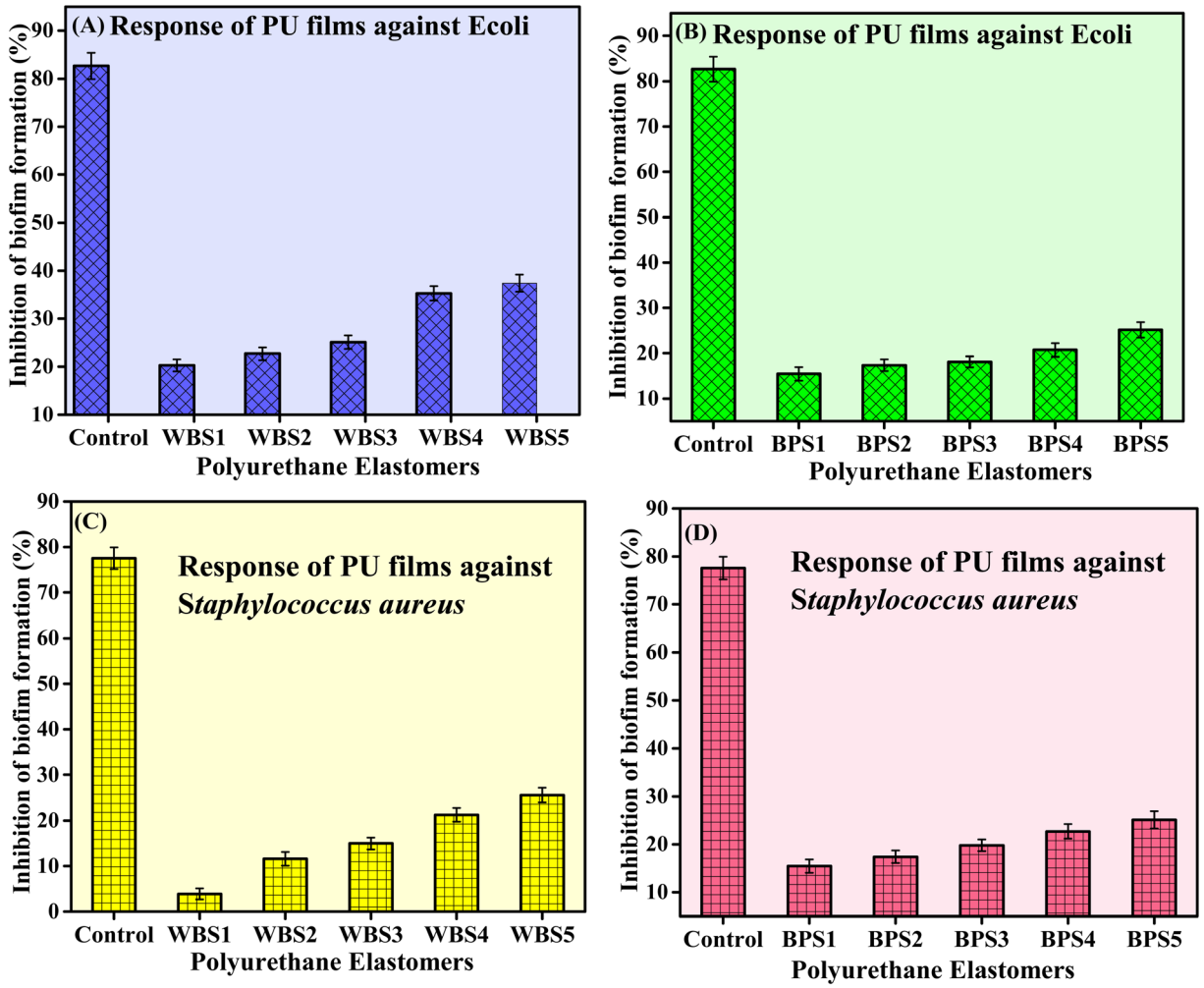

Fig. 6 Inhibition of film formation data of PU elastomers. (A) Inhibition of film formation data of the PUWS series chain extended with wheat bran starch against *E. coli*. (B) Inhibition of film formation data of the PUBS series chain extended with banana peel starch against *E. coli.* (C) Inhibition of film formation data of the PUWS series chain extended with wheat bran starch against *S. aureus*. (D) Inhibition of film formation data of the PUBS series chain extended with banana peel starch against *S. aureus.*

elastomers have shown significant biofilm inhibition against *S. aureus* and *E. coli*. A continuous increase in the values of biofilm inhibition has been observed by the increase in the concentration of starch. The samples of both PUWS and PUBS series have better resistance against *E. coli.* These analyses have shown that a slight change in the architecture of PU can develop better properties for their use in biocompatible application. The data of all of the samples have been presented in Fig. 6.

3.4.3. Phase contrast microscopic analysis of PU elastomers. Phase contrast microscopic analysis of some selected samples of both series of PU samples have been shown against *E coli* in Fig. 7. The figure has represented the dense, compacted growth of bacteria in the case of the negative control sample, which has been developed due to crystal violet. In contrast, a very clear image without a dense area or globulus has been observed in the case of the positive control bacteria. Fig. 11 shows the images of PUWS 2 and PUWS 4 which clearly shows the image resembling the that of the positive control bacteria. This information has strengthened the view that the samples have inhibited the microbial biofilm growth. The similar images have also been observed for PUBS2 and PUBS 5 samples, indicating the samples of PU elastomers have exhibited the inhibition of bacterial growth. Hence, the samples of both films have shown biocompatibility, and the PU elastomers can be utilized for biomedical applications. Fig. 8 shows the phase contrast microscopy analysis for PUWS and PUBS series against the bacterial growth of *S aureus*. Similar to the analysis of biofilm inhibition of *E. coli*, the negative control samples have shown condensed structure of microbial biofilm as compared to positive control sample whereas the samples of both series have shown biofilm inhibition properties. This is a clear indication that the synthesized samples are biocompatible materials and can be conveniently used for biofilm inhibition properties.

3.5. Analysis of mechanical/viscoelastic behavior of PU elastomers by DMA

DMA has been used to characterize the viscoelastic behavior of the PU elastomers as a function of temperature. The mechanical behavior plays a key role in deciding the strength and market value of the polymers. The mechanical behavior of the PU elastomers synthesized in series PUWS and PUBS has been reported in terms of the storage modulus (E') at 50 °C. The representative curves of E' with respect to temperature is given in Fig. 9. The E' is the ability of the polymer to store the energy elastically. It is a very important parameter for elastomers. The increase in the E' indicates a slightly stiff material, indicating an organized glassy state. The increase in the values of E' has been observed with the increase in the HS contents of the PU elastomer, as induced by the incorporation of diisocyanate and chain extender, whereas the starch has been reported by the researchers to be in the form of granules and partially crystalline in texture. The maximum modulus of 4.25 MPa has been observed in the PUWS series, whereas the PUBS series showed a significantly high E' as compared to the PUWS series. This is an indication of the elastic dominance and the presence of the physical entanglements in the polymers. As the physical entanglements will be affected with the temperature increase; hence, the decrease in E' is obvious. A similar behavior of decrease in the E' by the increase in the temperature has also been reported by Zhang *et al.*[47] in PU elastomers in connection

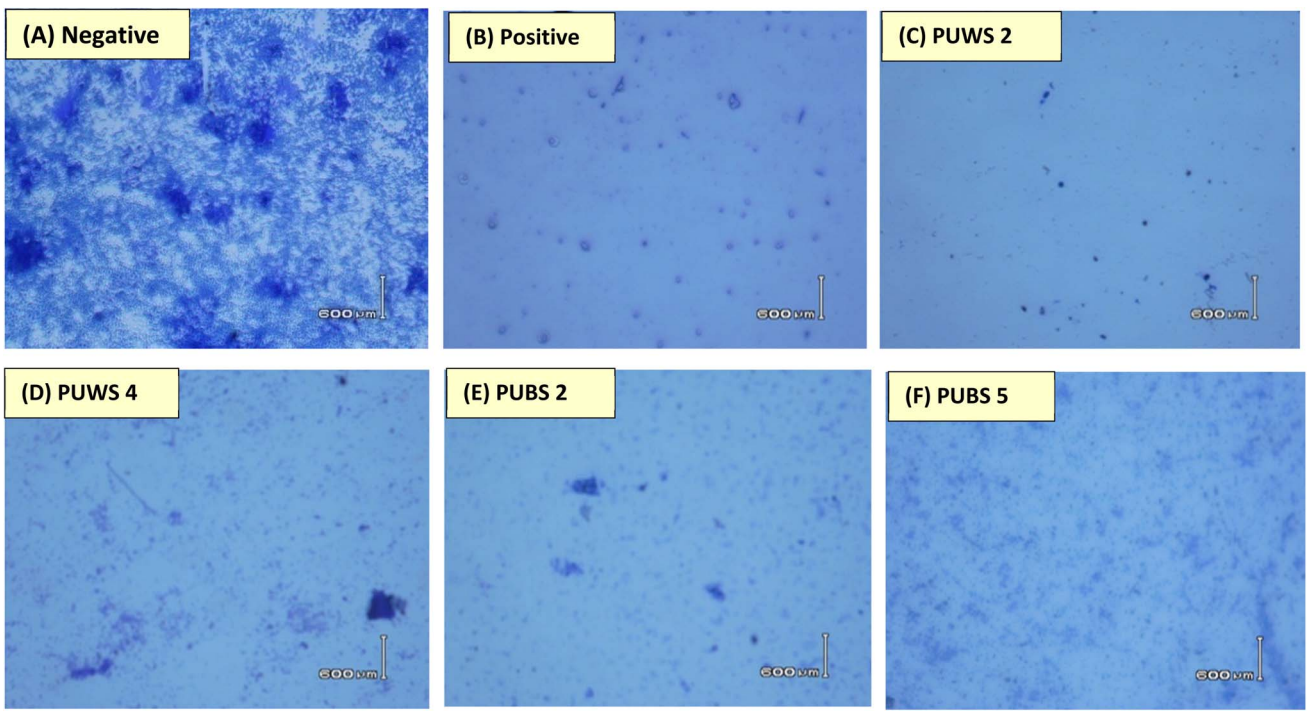

Fig. 7 Phase contrast microscopy images of the pattern of bacterial biofilm formation and its inhibition. (A) Negative growth, (B) positive control, (C and D) PUWS samples treated slides against the *E. coli* biofilm, (E and F) PUBS samples-treated slides against the *E. coli* biofilm.

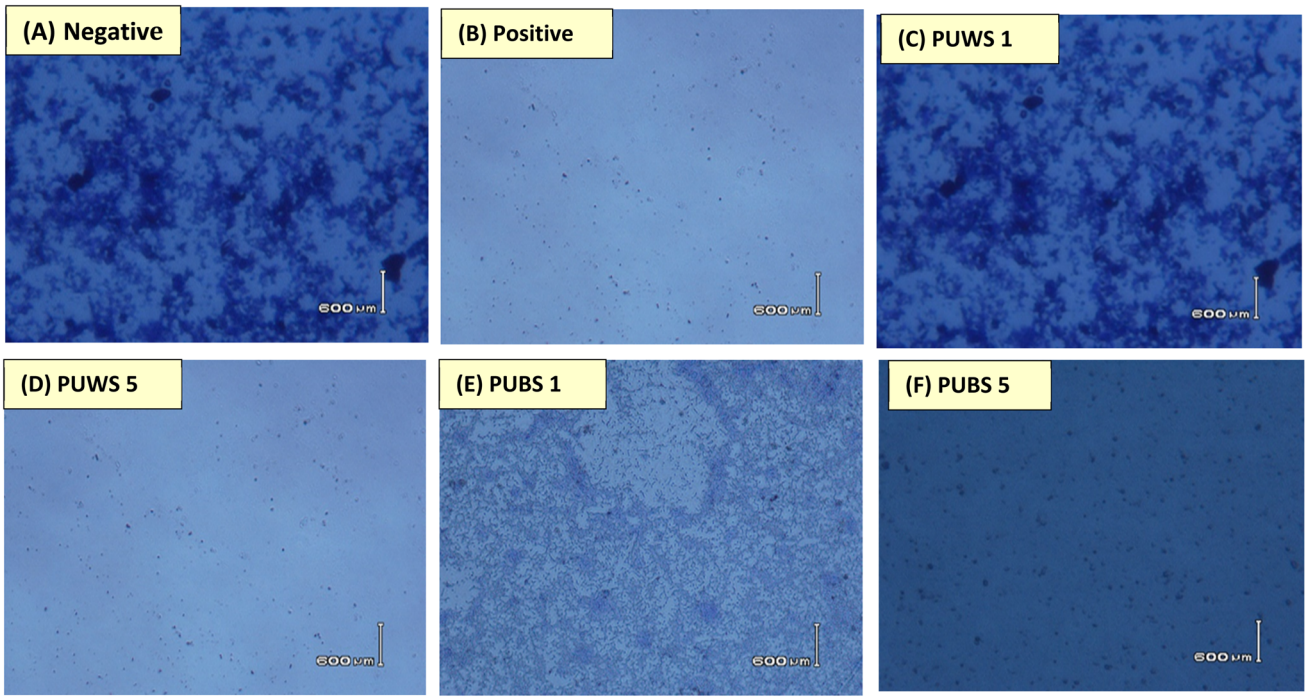

Fig. 8 Phase contrast microscopy images of the pattern of the bacterial biofilm formation and its inhibition. (A) Negative growth, (B) positive control, (C and D) PUWS samples-treated slides against *S. aureus*, (E and F) PUBS samples-treated slides against *S. aureus*.

with the effect of HS. Fig. 9 represents a relationship between tan δ and temperature. The viscoelastic behavior of the materials can be expressed as a ratio of loss modulus (E'') and E', which indicates the stored energy in the elastic portion and the energy dissipation as heat. This ratio of E'' to E' is represented as tan δ, which is known as the loss tangent or the tangent of phase

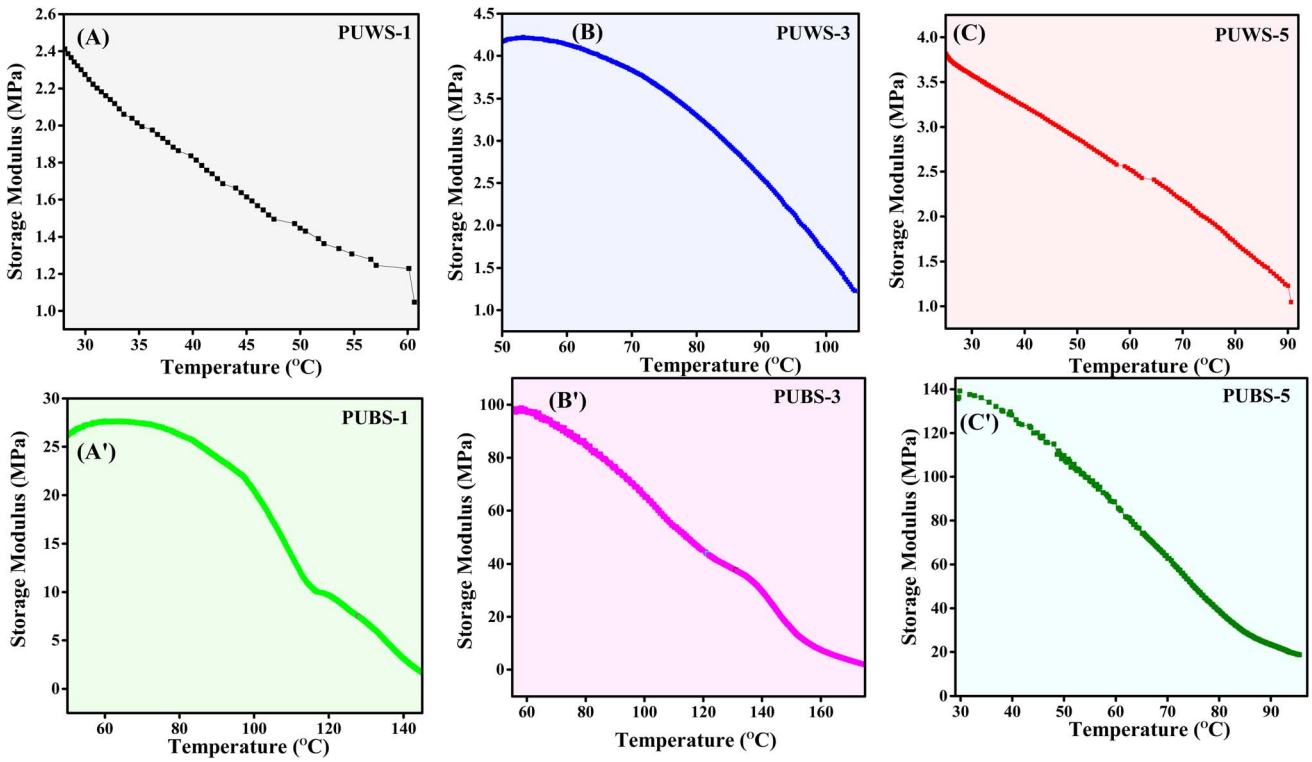

Fig. 9 Representative DMA curves showing the relationship between the storage modulus and temperature of some selected synthesized samples of the PUWS series chain extended with wheat bran starch and the PUBS series chain extended with banana peel starch.

angle between E' and E''. It provides a damping measure of the polymers. The damping factor has provided the information about the dissipation of energy from the PU elastomers under cyclic load. It has provided information about how the elastomer shed off the energy, and it has provided clear information about the absorption of energy by the elastomers. The temperature plays a key role in the absorption, as well as in the dissipation of the energy. Fig. 10 has shown an increase in the values of tan δ against temperature. The dissipated part of the energy is due to segmental motions of the polymer chains. The test revealed that the dissipation of energy in tan δ represents the ratio of the viscous-to-elastic response of a viscoelastic material, or the energy dissipation potential of a material. When the cyclic load is applied onto the polymers, a portion of the applied load follows the mechanism of energy dissipation, which occurs usually in the bulk parts of the polymers due to segmental motion of polymer chains. Meanwhile, the other part of the bulk polymers releases the load upon removal of the load, showing the elastic response. The value of tan δ is also associated with vibration damping, which requires large values of tan δ. The tan δ can provide information about the flexibility and the interactions of the chains. The area under the curves provides the information about the absorbed energy of polymer. A greater area under the curve results in greater mobility, which in turn, provides improved damping properties. This is a clear indication that the material can better absorb and dissipate energy. As the elastomers for any application are usually marked with better energy dissipation, the similar trend has been reported by Mostafavi *et al.*,[48] while they have synthesized the PU elastomer for vascular tissue engineering. Fig. 10 shows the increase in the values of tan δ with temperature, indicating the more viscous behavior of the PU elastomers with temperature. As a result, the samples have greater energy dissipation potential. The prime difference in the mechanical properties is due to the sources of raw materials. Hence, we find a huge difference in the mechanical behavior of the PU composites. Fig. 11 represents the relationship between the stiffness and temperature of the PUWS and PUBS series. The elastomers do not show high stiffness, and are usually marked with low stiffness. The addition of fillers however can significantly increase the stiffness of the polymers. There is only a slight change in the stiffness that has been observed. However, the lower stiffness does not affect the mechanical behavior of the polymers. The high stiffness has been recorded by the researchers with aramid nanofibers. One of the important features in the addition of the stiffness has been observed due to excessive hydrogen bonding, indicating that the stiffness can be increased by the addition of the secondary forces. However, the introduction of the biomaterials is not really meant for the increase in the mechanical behavior. Hence, the comparable mechanical properties can be obtained, as shown from the figure. Ideally, the mechanical strength should be determined at the same temperature. However, a slightly better mechanical strength has been observed with a slight variation in temperature for some samples, which can be related to the stoichiometric precision of the sample compositions.

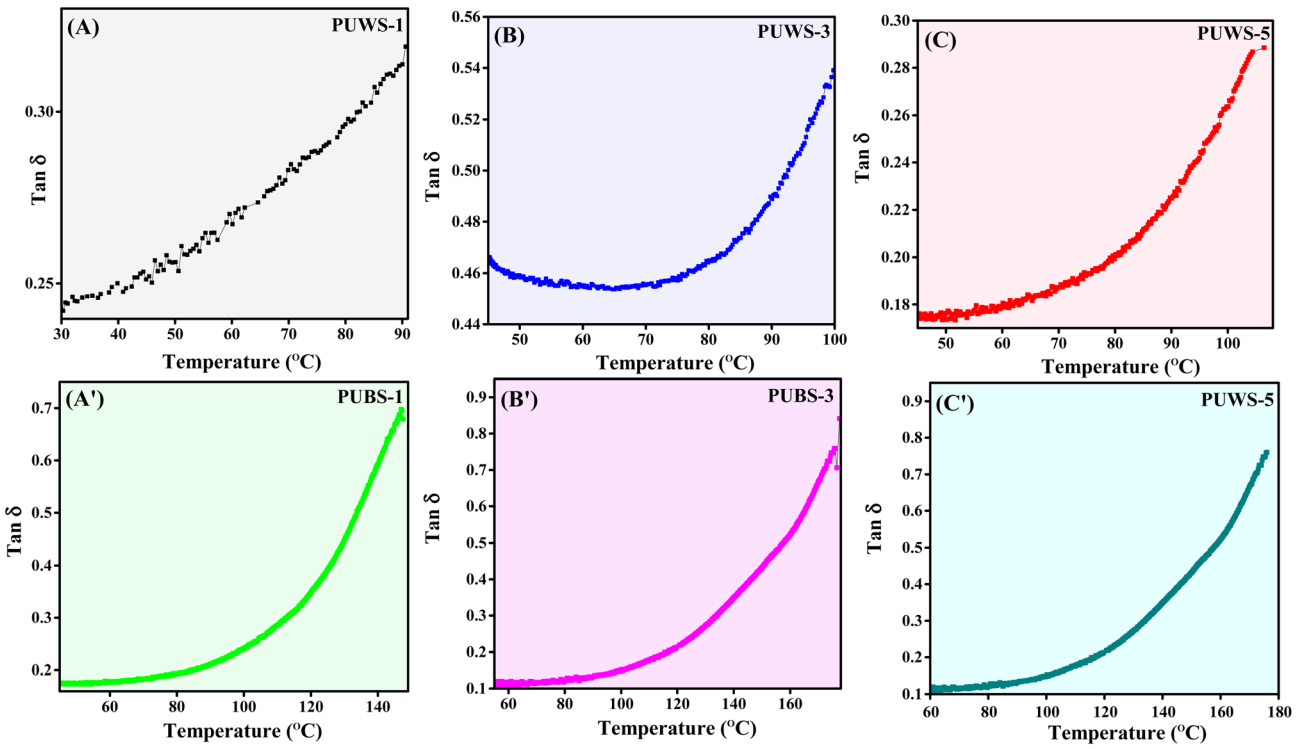

Fig. 10 Representative DMA curves showing the relationship between tan δ and the temperature of some selected synthesized samples of the PUWS series chain extended with wheat bran starch and the PUBS series chain extended with banana peel starch.

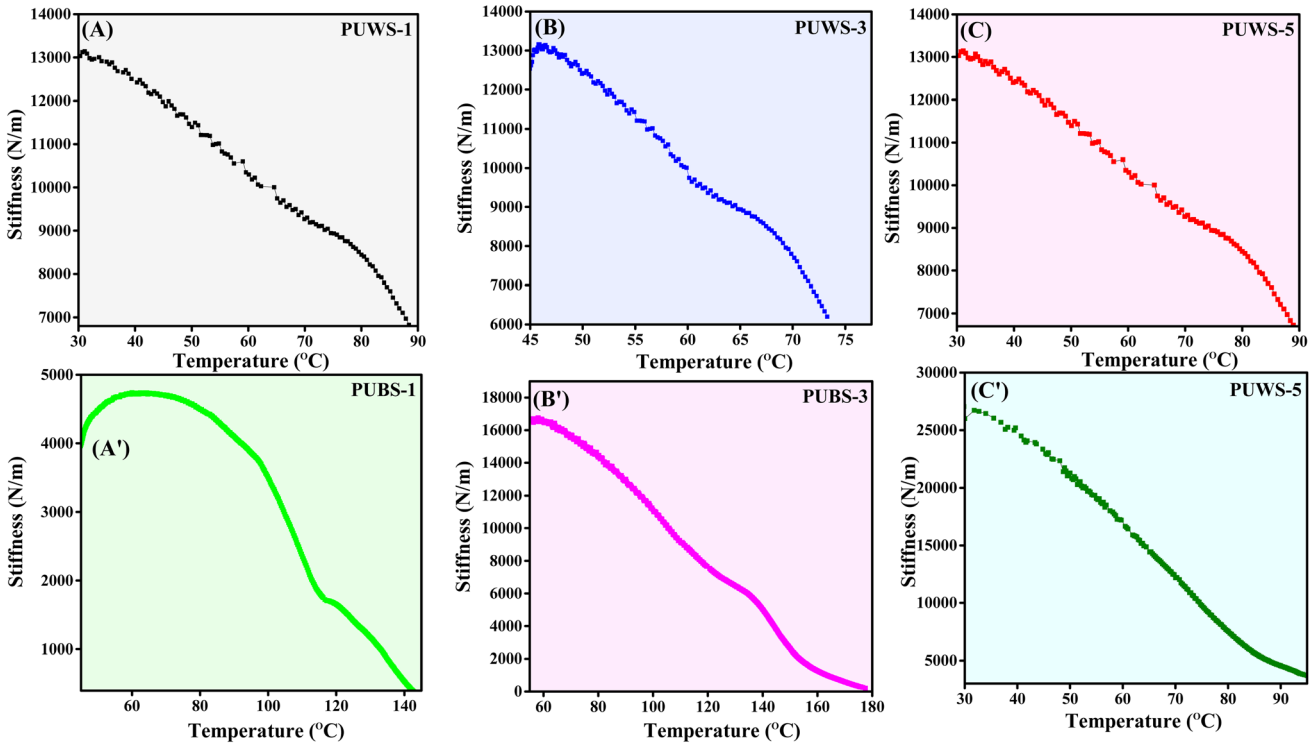

Fig. 11 Representative DMA curves showing the relationship between the stiffness and temperature of some selected synthesized samples of the PUWS series chain extended with wheat bran starch and the PUBS series chain extended with banana peel starch.

4. Conclusion

The bio-based polyurethane is attracting significant attention in the polymer industry. It is gaining interest not only because of environmental concerns, but it shows vibrant properties when analyzed in detail. It should be advantageous to replace any composite of the polymers with bio-based materials in order to induce comparable properties. In the current work, the elastomers of PU have been synthesized using the PEG macrodiol along with IPDI using prepolymer formation method. The NCO-terminated chains were extended using starch. The starch was extracted from wheat bran and banana peel. The ratio of the hard segment was varied from 40 to 70 wt%. Two series of PU elastomers were prepared by varying the source of starch as the chain extender in two different series, while the chain extenders were extracted from the raw materials of wheat bran and banana peel as bioresources. The FTIR analysis showed the disappearance of the characteristic peaks of NCO at 1750 cm^{-1}. The thermal stability was observed above 250 °C, whereas the maximum weight loss was observed above 400 °C. This indicates that by the addition of bio-components, a slight difference prevails in the thermal properties of the polymers, which can be tolerated easily for many applications. The DMA analysis showed that the elastomers of the PUBS series showed significantly higher E' of 140 MPa as compared to the PUWS series. A similar trend was observed in tan δ, where all of the values were observed ≤ 1, indicating significant elasticity in the samples. The elastomers showed significant stiffness behavior, which was a clear depiction of the mechanical strength of the elastomers. The hydrophilicity was observed through the swelling test. The greater hydrophilicity of the samples was observed up to 84 ± 1.0 (%) in the PUWS samples with a maximum concentration of the hard segment up to 72 (wt%). The DMSO, however, showed greater penetration of up to 88 ± 1.0 (%). The *in vitro* biological activities revealed the hemolytic activities of all PU elastomers within a safe range The inhibition of film formation was observed against *E. coli* and *S. aureus*, which revealed the optimum values of 37.40 ± 0.8 and 25.60 ± 0.7 (%) for the PUWS series. The results of the inhibition of the biofilm formation were also observed by using Phase contrast microscopy, which revealed the same finding.

Data availability

Data will be available on request.

Conflicts of interest

The authors declare no conflict of interest.

Acknowledgements

The authors extend their appreciation to the Researchers Supporting Project, King Saud University, Riyadh, Saudi Arabia, for funding this work through grant no. RSPD2023R566.

References

1 M. A. Javaid, K. M. Zia, A. Iqbal, S. Ahmad, N. Akram, X. Liu, H. Nawaz, M. K. Khosa and M. Awais, Synthesis and molecular characterization of chitosan/starch blends based polyurethanes, *Int. J. Biol. Macromol.*, 2020, **148**, 415.

2 N. Akram, S. Saleem, K. M. Zia, M. Saeed, M. Usman, S. Maqsood, N. Mumtaz and W. G. Khan, Stoichiometric-architectural impact on thermo-mechanical and morphological behavior of segmented Polyurethane elastomers, *J. Polym. Res.*, 2021, **28**, 1–15.

3 M. Y. Khalid, Z. U. Arif, W. Ahmed and H. Arshad, Recent trends in recycling and reusing techniques of different plastic polymers and their composite materials, *Sustainable Mater. Technol.*, 2022, **31**, e00382.

4 X. Shang, X. Fu, L. Yang and X. Chen, Structure and water absorption of starch and polyethylene-octene elastomer composites, *J. Reinf. Plast. Compos.*, 2008, **27**, 375–391.

5 N. Akram, R. S. Gurney, M. Zuber, M. Ishaq and J. L. Keddie, Influence of Polyol Molecular Weight and Type on the Tack and Peel Properties of Waterborne Polyurethane Pressure-Sensitive Adhesives, *Macromol. React. Eng.*, 2013, **7**, 493–503.

6 A. Cassales, L. A. Ramos and E. Frollini, Synthesis of bio-based polyurethanes from Kraft lignin and castor oil with simultaneous film formation, *Int. J. Biol. Macromol.*, 2020, **145**, 28–41.

7 F. Xie, T. Zhang, P. Bryant, V. Kurusingal, J. M. Colwell and B. Laycock, Degradation and stabilization of polyurethane elastomers, *Prog. Polym. Sci.*, 2019, **90**, 211–268.

8 M. Zeng, L. Zhang and Y. Zhou, Effects of solid substrate on structure and properties of casting waterborne polyurethane/carboxymethylchitin films, *Polym*, 2004, **45**, 3535–3545.

9 R. Santayanon and J. Wootthikanokkhan, Modification of cassava starch by using propionic anhydride and properties of the starch-blended polyester polyurethane, *Carbohydr. Polym.*, 2003, **51**, 17–24.

10 Z. U. Arif, M. Y. Khalid, M. F. Sheikh, A. Zolfagharian and M. Bodaghi, Biopolymeric sustainable materials and their emerging applications, *J. Environ. Chem. Eng.*, 2022, **10**, 108159.

11 Z. U. Arif, M. Y. Khalid, R. Noroozi, M. Hossain, H. H. Shi, A. Tariq, S. Ramakrishna and R. Umer, Additive manufacturing of sustainable biomaterials for biomedical applications, *Asian. J. Pharm. Sci.*, 2023, **18**(3), 100812.

12 M. Y. Khalid and Z. U. Arif, Novel biopolymer-based sustainable composites for food packaging applications: A narrative review, *Food Packag. Shelf Life*, 2022, **33**, 100892.

13 M. Ghasemlou, F. Daver, E. P. Ivanova, R. Brkljaca and B. Adhikari, Assessment of interfacial interactions between starch and non-isocyanate polyurethanes in their hybrids, *Carbohydr. Polym.*, 2020, **246**, 116656.

14 E. Dornez, K. Gebruers, S. Wiame, J. A. Delcour and C. M. Courtin, Insight into the distribution of arabinoxylans, endoxylanases, and endoxylanase inhibitors in industrial wheat roller mill streams, *J. Agric. Food Chem.*, 2006, **54**, 8521–8529.

15 S. Apprich, O. Tirpanalan, J. Hell, M. Reisinger, S. Böhmdorfer, S. S. Ehn, S. Novalin and W. Kneifel, Wheat bran-based biorefinery 2: Valorization of products, *LWT–Food Sci. Technol.*, 2014, **56**, 222–231.

16 M. Prueckler, S. Siebenhandl-Ehn, S. Apprich, S. Hoeltinger, C. Haas, W. Schmid and W. Kneifel, Wheat bran-based biorefinery 1: Composition of wheat bran and strategies of functionalization, *LWT–Food Sci. Technol.*, 2014, **56**, 211–221.

17 Z. M. Mosa and A. F. Khalil, The effect of banana peels supplemented diet on acute liver failure rats, *Ann. Agric. Sci.*, 2015, **60**, 373–379.

18 D. Prashanthi and M. Chaitanya, A review on multiple uses of banana peel, *J. Phys.: Conf. Ser.*, 2020, **5**, 120–122.

19 Z. Li, K. Guo, L. Lin, W. He, L. Zhang and C. Wei, Comparison of physicochemical properties of starches from flesh and peel of green banana fruit, *Molecules*, 2018, **23**, 2312.

20 M. A. Javaid, M. Asif, K. M. Zia, R. A. Khera, C. Jabeen, I. Mumtaz, M. Adnan, M. Younis, M. Shoaib and I. A. Bhatti, Evaluation of cytotoxicity, hemocompatibility and spectral studies of chitosan assisted polyurethanes prepared with various diisocyanates, *Int. J. Biol. Macromol.*, 2019, **129**, 116–126.

21 H. Joo and S. Cho, Comparative studies on polyurethane composites filled with polyaniline and graphene for DLP-type 3D printing, *Polym*, 2020, **121**, 67.

22 N. Akram, K. M. Zia, M. Saeed, M. Usman and W. G. Khan, Role of isophorone diisocyanate in the optimization of adhesion tendency of polyurethane pressure sensitive adhesives, *J. Appl. Polym. Sci.*, 2019, **136**, 47124.

23 S. Oprea, D. Timpu and V. Oprea, Design-properties relationships of polyurethanes elastomers depending on diferent chain extenders structures, *J. Polym. Res.*, 2019, **26**, 117.

24 Z. U. Arif, M. Y. Khalid, R. Noroozi, A. Sadeghianmaryan, M. Jalalvand and M. Hossain, Recent advances in 3D-printed polylactide and polycaprolactone-based biomaterials for tissue engineering applications, *Int. J. Biol. Macromol.*, 2022, **218**, 930–968.

25 M. Y. Khalid, A. A. Rashid, Z. U. Arif, W. Ahmed, H. Arshad and A. A. Zaidi, Natural fiber reinforced composites: Sustainable materials for emerging applications, *Results Eng.*, 2021, **11**, 100263.

26 M. P. Sudhakar, V. Nallasamy, G. Dharani and A. Buschmann, Applications of seaweed biopolymers and its composites in dental applications, *J. Appl. Biol. Biotechnol.*, 2023, 1–7.

27 P. S. Muthiyal and B. Purushothaman, Fabrication and characterization of stimuli responsive scaffold/bio-membrane using novel carrageenan biopolymer for biomedical applications, *Bioresour. Technol. Rep.*, 2023, **21**, 101344.

28 V. O. Sachin and P. J. Jyoti, *Seaweed-Based Biodegradable Biopolymers, Composite, and Blends with Applications. Bioremediation Using Weeds*, 2021, ISBN: 978-981-33-6551-3.
29 P. Y. Freile and S. T. J. Madera, *Biodegradable Polymer Blends and Composites from Seaweeds*, 2017, DOI: 10.1002/9781119441632.ch98.
30 M. P. Sudhakar, S. Venkatnarayanan and G. Dharani, Fabrication and characterization of bio-nanocomposite films using κ-Carrageenan and Kappaphycus alvarezii seaweed for multiple industrial applications, *Int. J. Biol. Macromol.*, 2022, **31**(219), 138–149, DOI: 10.1016/j.ijbiomac.2022.07.230.
31 N. Akram, I. Shahzadi, K. M. Zia, M. Saeed, A. Ali, R. Al-Salahi, H. A. Abuelizz and F. Verpoort, Fabrication and *In Vitro* Biological Assay of Thermo-Mechanically Tuned Chitosan Reinforced Polyurethane Composites, *Molecules*, 2023, **28**, 7218, DOI: 10.3390/molecules28207218.
32 H. Marta, Y. Cahyana, M. Djali and G. Pramafisi, The Properties, Modification, and Application of Banana Starch, *Polymers*, 2022, **14**, 3092, DOI: 10.3390/polym14153092.
33 R. Jana van, S. Senay, A. O. Samson and M. Marena, Wheat starch structure–function relationship inbreadmaking: A review, *Compr. Rev. Food Sci. Food Saf.*, 2023, **22**, 2292–2309.
34 K. H. Kim and J. Y. Kim, Understanding Wheat Starch Metabolism in Properties, Environmental Stress Condition, and Molecular Approaches for Value-Added Utilization, *Plants*, 2021, **10**, 2282, DOI: 10.3390/plants10112282.
35 F. Zia, K. M. Zia, M. Zuber, S. Kamal and N. Aslam, Starch based polyurethanes: A critical review updating recent literature, *Carbohydr. Polym.*, 2015, **134**, 784–798.
36 N. L. Tai, R. Adhikari, R. Shanks and B. Adhikari, Starch-polyurethane Films Synthesized Using Polyethylene Glycol-Isocyanate (PEG-Iso): Effects of Molecular Weight, Crystallinity, and Composition of PEG-Iso on Physiochemical Characteristics and Hydrophobicity of the Films, *Food Packag. Shelf Life*, 2017, **14**, 116–127.
37 C. Gürses, M. G. Karaaslan-Tunç, Ü. Keleştemur, S. Balcıoğlu, S. Gülgen, S. Köytepe, *et al.*, Aliphatic Polyurethane Films Based on Hexamethylene Diisocyanate and Saccharides for Biocompatible Transparent Coating on Optic Medical Devices, *Starch*, 2022, **74**(3–4), 2100214.
38 N. Akram, M. Saeed, M. Usman, A. Mansha, F. Anjum, K. M. Zia, I. Mahmood, N. Mumtaz and W. G. Khan, Infuence of graphene oxide contents on mechanical behavior of polyurethane composites fabricated with diferent diisocyanates, *Polym*, 2021, **30**, 444.
39 T. Shahzadi, M. Zaib, T. Riaz, S. Shehzadi, M. A. Abbasi and M. Shahid, Synthesis of Eco-friendly Cobalt Nanoparticles Using *Celosia argentea* Plant Extract and their Efficacy Studies as Antioxidant, Antibacterial, Hemolytic and Catalytical Agent, *Arabian J. Sci. Eng.*, 2019, **44**, 6435–6444.
40 K. Rubab, A. A. Muhammad, A. Rehman, S. Z. Siddiqui, S. A. A. Shah, M. Ashraf, Q. Ain, I. Ahmad, M. A. Lodhi, M. Ghufran, M. Shahid and H. Fatima, Synthesis, pharmacological screening and computational analysis of some 2-(1*H*-Indol-3-yl)-*N*′-[(un)substituted phenylmethylidene] acetohydrazides and 2-(1*H*-Indol-3-yl)-*N*′-[(un)substituted benzoyl/2-thienylcarbonyl] acetohydrazides, *Pak. J. Pharm. Sci.*, 2017, **30**, 1263–1274.
41 M. Shahid, H. Munir, N. Akhter, N. Akram, F. Anjum, Y. Iqbal and M. Afzal, Nanoparticles encapsulation of *Phoenix dactylifera* (date palm) mucilage for colonic drug delivery, *Int. J. Biol. Macromol.*, 2021, **191**, 861–871.
42 S. A. Shahid, F. Anwar, M. Shahid, N. Majeed, M. Azam, M. Bashir, M. Amin, Z. Mahmmod and I. Shakir, Laser-assisted synthesis of $Mn_{0.50}Zn_{0.50}Fe_2O_4$ nanomaterial: Characterization and *in vitro* inhibition activity towards *Bacillus subtilis* biofilm, *J. Nanomater.*, 2015, **44**, 1–6.
43 N. Akram, M. Usman, S. Haider, M. S. Akhtar and K. Gul, Impact of Diisocyanates on Morphological and *In Vitro* Biological Efficacy of Eco-Friendly Castor-Oil-Based Water-Borne Polyurethane Dispersions, *Polym*, 2022, **14**, 3701.
44 N. Qasim, M. Shahid, F. Yousaf, m. Riaz, F. Anjum, M. A. Faryad and R. Shabbir, Therapeutic Potential of Selected Varieties of Phoenix Dactylifera L. Against Microbial Biofilm and Free Radical Damage to DNA, Dose, *Response*, 2020, **18**, 1559325820962609.
45 J. Chen, R. Dong, J. Ge, B. Guo and P. X. Ma, Biocompatible, Biodegradable, and Electroactive Polyurethane-Urea Elastomers with Tunable Hydrophilicity for Skeletal Muscle Tissue Engineering, *ACS Appl. Mater. Interfaces*, 2015, **7**, 28273–28285.
46 P. Parcheta, E. Głowińska and J. Datta, Effect of bio-based components on the chemical structure, thermal stability and mechanical properties of green thermoplastic polyurethane elastomers, *Eur. Polym. J.*, 2020, **123**, 109422.
47 L. Zhang, L. Chen and S. J. Rowan, Trapping Dynamic Disulfide Bonds in the Hard Segments of Thermoplastic Polyurethane Elastomers, *Macromol. Chem. Phys.*, 2018, **2017**, 1600320.
48 A. Mostafavi, H. Daemi, S. Rajabi and H. Baharvand, Highly tough and ultrafast self-healable dual physically crosslinked sulfated alginate-based polyurethane elastomers for vascular tissue engineering, *Carbohydr. Polym.*, 2021, **257**, 117632.
49 N. Akram, K. M. Zia, M. Saeed, A. Mansha and W. G. Khan, Morphological studies of polyurethane based pressure sensitive adhesives by tapping mode atomic force microscopy, *J. Polym. Res.*, 2018, **25**, 194.
50 J. N. BeMiller, *Carbohydrate Chemistry for Food Scientists*, Woodhead Publishing and AACC International Press, London, UK, 3rd edn, 2018.
51 C. J. Doona, F. E. Feeherry and M. Y. Baik, Water Dynamics and Retrogradation of Ultrahigh Pressurized Wheat Starch, *J. Agric. Food Chem.*, 2006, **54**, 6719–6724.
52 Z. Yang, S. Chaib, Q. Gu and Y. Hemar, Impact of Pressure on Physicochemical Properties of Starch Dispersions, *Food Hydrocolloids*, 2017, **68**, 164–177.
53 J. N. BeMiller, Preface to the Third Edition in *Starch: Chemistry and Technology*, (Food Science and Technology), ed. BeMiller J. and Whistler R., Academic Press, San Diego, CA, USA, 3rd edn, 2009, pp. xvii–xviii.